Transient Flux Dynamics in Optically Irradiated YBCO Thin-Film Switches

Fast switching using thin films of high-temperature superconductor (HTS) has been a subject of interest in recent years. Several high-power applications, including fault current limiters, generation of fast current pulses, and energy extraction from superconducting magnetic energy storage (SMES), require an opening switch with high current-carrying capacity and fast rise times. The property requirements of the opening switch are diverse and depend on the application.[1] In this article, we discuss a contactless, inductively coupled opening switch that employs $YBa_2Cu_3O_{7-x}$ (YBCO) thin films.

In its simplest form, the switch consists of a film of HTS placed between the primary and secondary coils of a transformer, shown conceptually in Fig. 61.15.[2] A current source drives current in the primary coil. If the film is superconducting, it screens the magnetic flux, and there is no flux coupling between the two coils. If a load is connected across the secondary coil, the voltage across the load is zero. Upon illumination by a laser pulse, the film makes a transition to the normal state, allowing magnetic flux produced by the primary current to couple into the secondary coil. The temporal change of flux through the secondary coil results in an induced voltage $(V = -\partial\Phi/\partial t)$ across the load. A similar contactless arrangement has been used to measure critical temperature and critical current density of films.[3] Optically thick films (500–800 nm) were used in our experiment to enhance the current-carrying capacity. A ring of 5-mm width, 1-mm thickness, and 20-MA/cm^2 current density will correspond to a current of 1 kA that can produce a field $(B = \mu_0 I/2a)$ of about 0.12 T at the center of the ring. This order-of-magnitude estimate suggests that a large field can be excluded using thin films with very high critical current density (J_c).

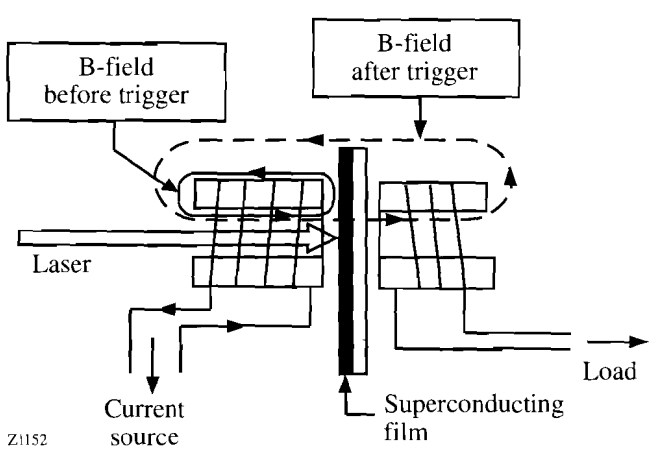

Figure 61.15
A conceptual diagram of the high-temperature superconducting thin-film switch. The superconducting film acts as a magnetic shield until triggered.

Figure 61.16 shows the configuration of our switching system, which has three components: the source (the primary coil in our discussion), the switch (the superconducting film), and the load circuit (the secondary coil and load). The superconducting magnet serves as the primary coil (source), while two superconducting films (switch) are placed on either side of the secondary coil.

Theory

For the described switch configuration, if the applied field, which is perpendicular to the film surface, is below the lower critical field (H_{c1}) of the superconductor, the superconductor is in a reversible Meissner state and will initially screen the flux produced by the magnet from coupling to the secondary coil. When it is driven to its normal state by heating with a laser pulse, the magnetic flux moves radially inward and produces a voltage pulse across the secondary coil. As the film cools down and returns to its superconducting state, it will expel the flux. Repetitive switching can then be performed with a train of laser pulses.[2] If the applied field exceeds H_{c1}, the flux will still be excluded from the superconductor up to a certain field strength depending upon the critical current density of the film (critical state model). Beyond this point, only a partial flux exclusion will take place as the screening currents in the superconductor redistribute to exclude the flux from the center of the film. Single-shot switching can still be performed under these conditions, allowing the excluded flux to couple to the secondary coil. As the film cools into the superconducting

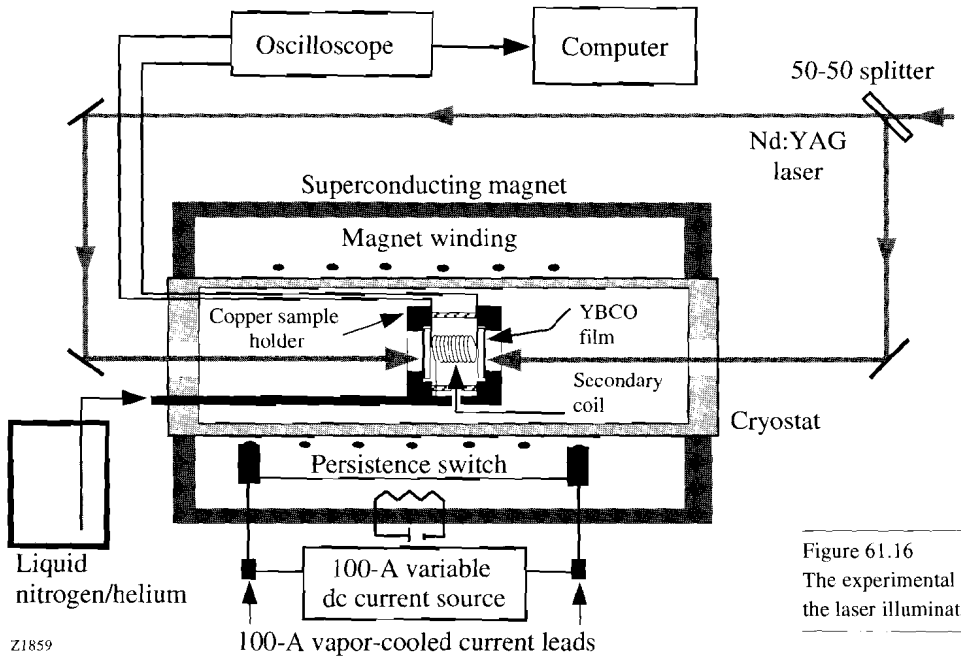

Figure 61.16
The experimental setup for the high-field experiments showing the laser illumination scheme and the data acquisition system.

state, however, it will no longer expel the penetrated flux. Because the thin-film geometry produces a large demagnetization factor that causes enhancement of the magnetic field at the edges of the film, some field penetration occurs at the edges, even when the applied field is less than H_{c1}.

To understand the motion of flux inside the superconductor following its transition into the normal state, we must analyze the distribution of screening currents and magnetic fields. Temporal variation of the flux in the secondary coil, which is inductively coupled to the superconducting films, must also be investigated.[4] We first calculate the current and field distribution in a film of thickness t, shaped like a circular disk of radius R, for a given externally applied field (B_{ext}) and critical current density (J_c) by dividing the disk into a set of n concentric circular strips of equal width ($w = R/n$, where $n = 25$ for our calculation). Starting from the current-density distribution $J(r)$ required for complete flux exclusion inside the film, the J_c-limited distribution is calculated iteratively. At each step of the iteration the field is allowed to penetrate from the edge by the width of one ring more than the previous step. If the field penetrates to a radius a, $J(r < a)$ is recalculated to make the region $0 < r < a$ flux free, and $J(r > a)$ is set equal to J_c. For a single film and field-independent critical current, our result, shown in Fig. 61.17, exactly matches the analytical expression given by Mikheenko and Kuzovlev.[5]

We then proceed to calculate the temporal evolution of current distributions in the two films and the secondary coil. This is done by treating each ring in the two films and the secondary coil as $(2n + 1)$ circuits. We then solve a set of linear equations of the form $[L]d[I]/dt + [R][I] = 0$, where $[L]$ and $[R]$ are matrices of dimension $(2n + 1) \times (2n + 1)$ and $[I]$ is a column vector. The diagonal elements of $[L]$ are the inductances of each circuit, and off-diagonal elements are the appropriate mutual inductances. $[R]$ is a diagonal matrix with elements equal to the normal-state resistances of the circuits. The elements of $[I]$ represent the current in each circuit. Using

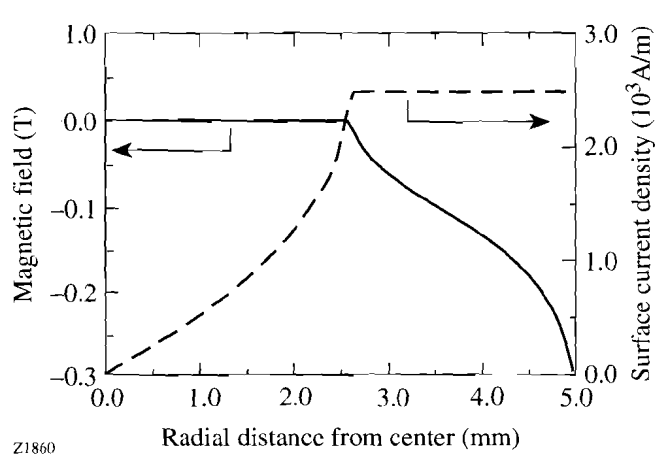

Figure 61.17
Static J_c-limited surface current and z-component of the magnetic field for a 1-cm-diam, thin superconducting disk of 500-nm thickness. A constant critical current density of 5.10^7 A/cm^2 and an externally applied field of −0.2 T are assumed.

this analysis we calculate the current in the secondary coil as a function of time; Fig. 61.18 shows the result of this calculation. The matrix formulation of the problem enables us to take advantage of the computationally efficient, matrix manipulation tools in commercial software packages such as MATLAB™. The numerical method discussed above can easily incorporate additional details,[4] e.g., field-dependent critical current densities $J_c(B)$ and field-dependent superconducting flux-flow resistances.

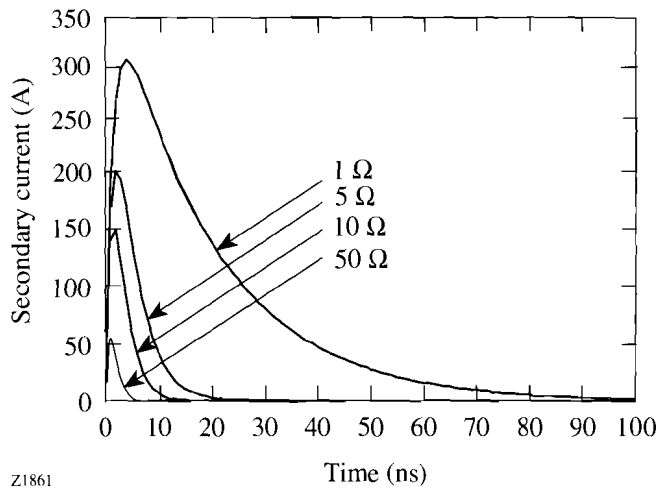

Figure 61.18
The simulated current pulse produced at a single-turn secondary coil for different values of load resistance. Two identical, 1-cm-diam, 500-nm-thick, disk-shaped superconducting films with $J_c = 5.10^7$ A/cm^2 are placed on either side of the secondary coil at a distance of 1 mm. The externally applied field (B_{ext}) is −0.2 T.

Experimental Results and Discussion

The magnet used in our experiment is a Nb-Ti solenoid cooled by liquid helium, rated at 100 A and a maximum field of 4 T. A schematic drawing of the entire experimental setup, including the cryostat and magnet, is shown in Fig. 61.16.

The secondary coil is a single-turn inductor patterned on a printed circuit board. The sample holder consists of two 2-in.-diam circular copper disks with 1-cm × 1-cm-sq windows. The films, 500-nm-thick YBCO on 1-cm × 1-cm $LaAlO_3$ substrates with $T_c > 88$ K, are placed on either side of the secondary coil and supported by the copper disks.

A Nd:YAG laser beam (λ = 1064 nm; pulse width = 150 ps) was used to illuminate the films from either side through a splitter arrangement (Fig. 61.16). A stainless steel, semirigid coaxial cable carries the secondary voltage signal out of the cryostat to a computer-interfaced oscilloscope for viewing (Fig. 61.16).

After cooling the sample to the desired temperature using liquid nitrogen or helium in zero magnetic field, the magnet was then charged at a ramp rate of 0.1 A/s up to the desired level and was maintained in persistent current mode. The magnetic field strength was measured using a Hall probe and a gaussmeter.

With the magnet charged, the switch was illuminated by the laser. The YBCO films screening the secondary coils were driven normal by this laser irradiation, which allowed the flux to penetrate. A secondary voltage (of negative sign) appeared across the load. The magnet was then discharged by heating the persistent switch, leaving some of the flux trapped in the superconductor. Driving the films normal again expelled the trapped flux, and the corresponding secondary voltage signal (of positive sign) was observed.

Figure 61.19 shows a comparison of the experimentally observed secondary voltage signal at an applied field of −0.2 T with the one obtained with the theoretical analysis described in the previous section. The simulation was done by varying J_c to match the flux associated with the output voltage pulse. The peak voltage of the simulated pulse is higher than the experimentally observed pulse because instantaneous transition to the normal slate was assumed. The critical current density required to match the flux was 1.33×10^6 A/cm^2, which

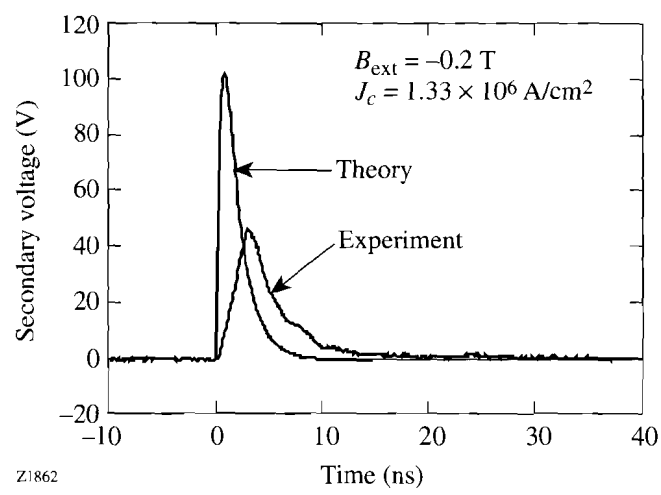

Figure 61.19
A comparison of experimentally obtained secondary voltage with the simulated voltage pulse representing the same flux. The experiment was carried out at 12.4 K, in −0.2-T field, and 8 mJ of laser energy per film.

is of the right order of magnitude but slightly lower than the value of J_c at zero field, as quoted by the film manufacturer. Possible sources of reduced effective J_c might include suppression in the magnetic field or sample inhomogeneity.

The variation of the secondary voltage signal for different laser energies is shown in Fig. 61.20. At lower laser energies, the entire bulk of the film is not heated instantaneously above the transition temperature. The 500-nm film thickness is greater than the optical penetration depth (≈120 nm); consequently the upper section of the film absorbs most of the energy when the laser pulse is incident on the film. The heat is eventually redistributed by diffusion, elevating the temperature of the entire film above the critical temperature. The heat is then redistributed throughout the remaining bulk of the film by thermal diffusion.[6] If we divide the film into a series of layers normal to the propagation direction of the incident laser radiation, the bottom layers will remain superconducting and carry the screening currents even after the top layers become nonsuperconducting. These screening currents continue to exclude flux and retard its motion. Since the secondary voltage is the temporal derivative of the flux, the peak voltage goes down, and rise and fall times increase, with the decrease in laser fluence. However, as shown in Fig. 61.20, the time integral of the secondary voltage pulse, representing the total flux that has traversed the film, is the same for pulses triggered by laser irradiation of varying intensity. Based on these results,

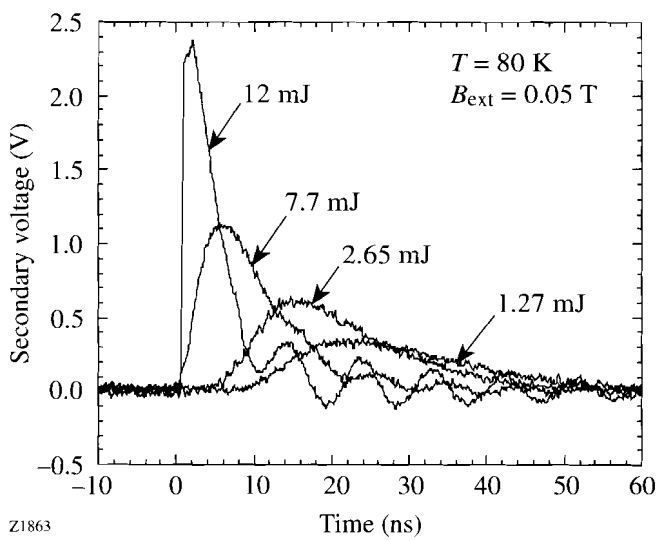

Figure 61.20
The speed of flux motion depends on the incident laser energy. For lower laser energy the bottom part of the film remains superconducting for a while, impeding the motion of flux. The film was a 1-cm-diam disk with a thickness of 500 nm.

we can conclude that higher laser fluence will give rise to faster signals with higher peak voltage. The energy (E) delivered to the load is given by $E = 1/R \int V^2(t)dt$, where R is the load resistance and $V(t)$ is the voltage across the secondary. For the same flux, $\Phi = \int V(t)dt$, a faster signal will deliver higher energy in the load. Both the peak voltage and the flux are larger at lower temperatures because J_c is higher.

An inductively coupled switch of the type we have described lends itself to a variety of applications. For example, in a current multiplication circuit using programmed inductive elements (PIE),[7] storage inductors are charged in series and discharged sequentially in stages that are connected in parallel with the load through a set of isolating closing switches. This circuit can be used to deliver a large load current using switches that are rated at a fraction of that current. The most important constraint in such a circuit is the synchronization of the opening switches with the closing switches. If the opening switches in this circuit are not triggered within a short temporal window, transient high current or voltages will catastrophically destroy the circuit elements. Optical triggering provides accurate timing. The optically triggered inductive opening switch will be suitable in circuits with such constraints.

The contactless arrangement of our switch is especially suited for applications such as energy extraction from SMES,[8–9] though there are some unresolved problems. The main application of SMES is as a backup source of energy to be delivered to the load in a crisis situation. If an opening switch is placed in series with the magnet winding, the finite closed-state resistance of the switch results in a continuous loss of energy while the system is idle. A contactless switch will solve this problem; the film properties, however, will need to be significantly improved for this design to be practical for high-power applications.

Conclusion

We have described the flux dynamics in a contactless opening switch. The switching is performed by the optical heating of YBCO thin films, which in their superconducting state screen the flux coupling between two inductively coupled circuits. A single-turn secondary coil with a small L/R time produces a fast voltage pulse. The rise time of the output signal is about 1 ns. At lower temperatures the critical currents are higher and can screen higher fields. Fast voltage pulses of 100 V and higher are possible and may have switching applications. We have developed a theoretical model, supported by experimental evidence, that can be used as a diagnostic tool to study flux motion.

ACKNOWLEDGMENT

This work was supported by BMDO through ONR Contract #N00014-92-J-1993, Rochester Gas and Electric, NSF Grant #DMR-9122727, the New York State Energy Research and Development Authority, and the Frank J. Horton Graduate Fellowship Program.

REFERENCES

1. E. M. Honig, in *Opening Switches*, edited by A. Guenther, M. Kristiansen, and T. Martin, Advances in Pulsed Power Technology, Vol. 1 (Plenum Press, New York, 1987), pp. 1–48.

2. D. Gupta, W. R. Donaldson, K. Kortkamp, and A. M. Kadin, IEEE Trans. Appl. Supercond. **3**, 2895 (1993).

3. J. H. Claassen, M. E. Reeves, and R. J. Soulen, Jr., Rev. Sci. Instrum. **62**, 996 (1991).

4. D. Gupta, W. R. Donaldson, and A. M. Kadin, submitted to the Journal of Applied Physics.

5. P. N. Mikheenko and Yu. E. Kuzovlev, Physica C **204**, 229 (1993).

6. D. Gupta, W. R. Donaldson, K. Kortkamp, and A. M. Kadin, in *Optically Activated Switching II*, edited by G. M. Loubriel (SPIE, Bellingham, WA, 1992), Vol. 1632, pp. 190–195.

7. T. Burke *et al.* (private communication); also presented at the IEEE's High Voltage Workshop, Monterey, CA, March 1988.

8. W. R. Donaldson, D. Gupta, and A. M. Kadin, U. S. Patent No. 5,339,062 (16 August 1994).

9. D. Gupta, W. R. Donaldson, and A. M. Kadin, in *Advances in Cryogenic Engineering*, edited by P. Kittel (Plenum Press, New York, 1994), Vol. 39, Part B, pp. 2015–2020.